



HAL
open science

Multistatic acoustic Doppler profilers for fine-scale studies of velocity and particle flux processes

David Hurther, Ulrich Lemmin

► **To cite this version:**

David Hurther, Ulrich Lemmin. Multistatic acoustic Doppler profilers for fine-scale studies of velocity and particle flux processes. 2nd International Conference & Exhibition on "Underwater Acoustic Measurements: Technologies & Results", 2007, Heraklion, Greece. pp.1027-1034. hal-00265850

HAL Id: hal-00265850

<https://hal.science/hal-00265850>

Submitted on 21 Jan 2020

HAL is a multi-disciplinary open access archive for the deposit and dissemination of scientific research documents, whether they are published or not. The documents may come from teaching and research institutions in France or abroad, or from public or private research centers.

L'archive ouverte pluridisciplinaire **HAL**, est destinée au dépôt et à la diffusion de documents scientifiques de niveau recherche, publiés ou non, émanant des établissements d'enseignement et de recherche français ou étrangers, des laboratoires publics ou privés.

Multistatic acoustic Doppler profilers for fine-scale studies of velocity and particle flux processes

D. Hurther⁽¹⁾, U. Lemmin⁽²⁾

⁽¹⁾ LEGI-CNRS, BP53, 38041 Grenoble cedex 9, France; david.hurther@hmg.inpg.fr

⁽²⁾ ENAC-LHE-EPF Lausanne, CH-1015 Lausanne, Switzerland ; ulrich.lemmin@epfl.ch

Although Acoustic Backscattering Systems (ABS) working in MHz range have proven their potential for small-scale flow studies under laboratory and field conditions, they are still subject to significant errors in the upper range of the turbulent energy spectrum (Thorne and Hanes 2002). Two novel methods improving the inversion of incoherent intensity and coherent pulse-to-pulse Doppler phase-shifts will be proposed and discussed: (a) the first method increases the stability of the inverted sediment concentration profile in the case where acoustic intensity attenuation can not be ignored such as observed in highly turbulent benthic regions. (b) The second one allows increasing the SNR in the turbulent energy spectra by suppressing that fraction of the Doppler noise which affects the inertial subrange. Both methods use quasi-simultaneous and co-located bi-frequency information obtained with a single emitter and a versatile hardware system. Validation experiments with fine particle suspensions are conducted in open-channel flows and for grid generated turbulence in a mixing box. The capacity of multi-frequency ABS to profile turbulent erosion fluxes is demonstrated.

Introduction

Acoustic Backscattering Systems (ABS) such as Acoustic Doppler Current Profilers (ADCP) and Acoustic Doppler Velocimeters (ADV) are intensively used among the oceanographic, coastal and nearshore research as versatile measuring tools for a wide range of studies addressing bio-geo-chemico-physical processes (Hamilton et al. 1998, Gilboy et al., 2000, Kim et al. 2000, Elgar et al., 2005, Betteridge et al. 2006). More recently, these instruments are increasingly employed in river, channel flow, lake and reservoir studies (Lane et al. 1998, Lopez and Garcia 1999, Hurther and Lemmin 2000, Nikora and Goring 2000, Blanckaert and DeVriend 2004, 2005, Bricault 2006, Hurther et al. 2007) for which current speed, discharge, suspended sediment concentration, water-depth or bed-topography information are aimed. The main advantage of acoustical devices is their ability to measure the flows characteristics in high turbidity conditions where optical tools can not be employed. Furthermore, unlike LDV or PIV systems, acoustical devices can be easily deployed in the field as autonomous instruments. Finally there is a tendency to choose ABS for suspension flow studies (Thorne and Hanes 2002) as the backscattered intensity can be inverted for sediment concentration estimations (Hamilton et al. 1998, Shen and Lemmin 1999, Admiraal and Garcia 2000, Fugate and Friedrichs 2002, Hurther and Lemmin 2003, Bricault 2006). This capability can be combined with velocity measurements in order to provide sediment flux profile estimates. The present study proposes improvements in pulse-to-pulse coherent velocity profiling and sediment concentration profiling at turbulent scales using a single emitter combined with a versatile hardware system. This system allows for quasi-simultaneous multi-frequency profiling in a co-located sample volume. The ability to perform erosion flux profiling in the benthic region of highly turbulent suspension flows is validated.

1. Acoustic intensity inversion for fine-scale suspension concentration profiling

We start from the expression of the output signal $I(r)$ of a monostatic ABS that is proportional to the acoustic intensity backscattered by a cloud of suspended particles located at a distance r from the transducer (Thorne and Hanes 2002). This expression is valid under the assumption of incoherent and first order (multiple scattering is neglected) scattering processes:

$$I(r) = \left[\left(\frac{RT_v P_o r_o}{1.05ka, \psi r} \right)^2 \frac{3\tau.c}{16} e^{-4\alpha_w r} \right] \left[\frac{\langle a_s^2 |f_m|^2 \rangle}{\langle a_s^3 \rangle \rho_s} \right] C(r) e^{-4 \int_0^r \zeta_s(r') C(r') dr'} \quad (1)$$

Where $R, T_v, P_0, r_0, k, a_b, \psi, r, \tau, \alpha_w, \zeta_s, a_s, f_m, \rho_s, C$, are the transducer constant, the hardware constant, the reference pressure at a reference distance, the reference distance, the wavenumber of the emitted ultrasound, the radius of the transducer, the transducer directivity function, the distance from the transducer, the duration of the emitted pulse train, the water attenuation constant, the sediment attenuation constant, the mean radius of the insonified particles, the mass concentration of the particle suspension.

In order to simplify the previous expression, we define three new variables as follows:

$$I_j = A_j A_s C_j e^{-4 \int_0^{r_j} \zeta_s(r) C(r) dr} \quad \text{With} \quad J_j = \frac{I_j}{A_j A_s} = C_j e^{-4 \int_0^{r_j} \zeta_s(r) C(r) dr} \quad (2)$$

Where j is the index of the gate located at $r=r_j$. A_j is the range dependent system parameter, A_s is the acoustic sediment parameter and J_j is the desired local sediment mass concentration affected by the non-linear sediment attenuation effect along the travel path of the acoustic pulse train. As will be shown below, this effect is at the origin of significant instabilities in the estimated concentration profile (Thorne and Hanes 2002).

In this study we consider that A_s is independent of range, since the studied suspension flows are all constituted of particles with mono-dispersed size distributions. Also note that $I(r)$ corresponds to the ABS output signal that is proportional to the mean square backscattered pressure. In section 4 we will investigate whether this expression can be applied to estimate suspension concentration at turbulent flow scales.

In the following two subsections we discuss the principles and performances of different inversion methods of Eq. (2) in order to extract the suspension concentration in benthic regions of highly turbulent suspension flows.

1.1 Iterative inversion method: principle and limitations

The iterative inversion method has been proposed by Thorne *et al.* (1993). In order to invert the normalized intensity J_j (see Eq. (2)) at a given point j , it is necessary to know the sediment concentration profile between the transducer and this point. Therefore, an iterative resolution from one point to the consecutive one is necessary: knowing the concentration at the first measuring point of the profile, the intensity attenuation between this point and the next one can be deduced. This implies a negligible attenuation between the transducer and the first point in order to determine the concentration at this first point, i.e.: $C_1 = J_1$. This boundary condition is a source of significant inversion errors when measuring in highly turbulent benthic suspension regions. The point to point iterative procedure becomes:

$$C_{j+1} = C_j \frac{J_{j+1}}{J_j} e^{4 \zeta_s \int_{r_j}^{r_{j+1}} C(r) dr} \quad (3)$$

Another difficulty in Eq. (3) is the incapacity to determine the exact value of the attenuation integral between two consecutive points in the profile. The integral can only be approximated by a numerical scheme. Using a rectangular method for the integral approximation, Eq. (3) becomes :

$$C_{j+1} = C_j \frac{J_{j+1}}{J_j} e^{4 \zeta_s C_j \Delta r} \quad (4)$$

As a result the iterative inversion method relies on the assumptions of negligible intensity attenuation due to the suspension between the transducer and the first point of the profile, and the discrete numerical estimate of the attenuation integral between consecutive points. In most cases errors linked to these two assumptions are cumulative. Indeed, if the concentration profile is monotonic along the transducer axis, the sign of the error in the estimation for each integral will be the same. This leads to an increase of the error with distance from the transducer. Furthermore, the integral estimate error propagates with the iteration steps. Thus even the smallest error at one point generates errors at all

following points in the profile. This is particularly severe when an error is made at the first point where attenuation is assumed to be negligible, because it will cause errors over the entire profile. The estimated suspension concentration will tend towards zero or infinity when the error is negative or positive, respectively. Therefore, this method is not well suited for attenuating media found in highly turbulent benthic suspension flows.

1.2 Explicit inversion method: principle and limitations

This method has been proposed by Lee and Hanes (1993). It relies on the analytical solution to Eq. (2) starting from the natural logarithm of this equation. After operating an adequate change of variable, its derivative with range r can be integrated and becomes:

$$C_j = \frac{J_j}{1 - 4\zeta_s \int_{r_1}^{r_j} J(r) dr} \quad (5)$$

As for the iterative inversion method it is assumed that intensity attenuation due to sediments between the transducer and the first point in the profile is negligible, i.e. that: $C_1 = J_1$.

Furthermore, the integral of the normalized intensity $J(r)$ also has to be approximated by a discrete numerical scheme. However, in this method, the numerical resolution of Eq. (5) will remain explicit for any type of numerical scheme that approximates the integral (rectangular or trapezoidal methods). It has to be noted that inversion instability problems are similar for all type of numerical scheme.

Adopting the same rectangular scheme for the integral approximation in both inversion methods, the local suspension concentration becomes:

$$C_j = \frac{J_j}{1 - 4\zeta_s \Delta r \sum_{i=1}^{j-1} J_i} \quad (6)$$

The problems here arise from the error affecting the denominator of Eq. (6). Both terms in the denominator are subject to errors. The error in the denominator term originates from the assumption $C_1 = J_1$ whereas the error in the second denominator terms is caused by the integral approximation.

When the assumption $C_1 = J_1$ is not valid at the first gate, the application of Eq.(6) will lead to underestimated concentrations whereas the errors in the approximations of the normalized intensity $J(r)$ will induce a singularity in the estimated concentration profile. Before the singularity, the inverted concentration will be overestimated. After the singularity it will become negative before reaching zero asymptotically with distance r from the transducer.

The previous analysis considered both effects separately. When both are taken into account the prediction of the total effect on the estimated concentration profile becomes impossible.

Finally, as for the iterative inversion method, the error propagates via the integral of the normalized intensity $J(r)$ between the second gate and the gate j . Thus a perturbation at one any gate of the profile will affect the subsequent concentration estimates.

1.3 A novel bi-frequency inversion method

In order to reduce the instabilities in the estimated concentration profiles we propose a bi-frequency inversion method. Starting from the following relation:

$$\frac{(J_{i,j})^{\zeta_{s_k}}}{(J_{k,j})^{\zeta_{s_i}}} = (C_j)^{\zeta_{s_k} - \zeta_{s_i}} \quad (7)$$

The concentration profile can be estimated from :

$$C_j = (J_{i,j})^{\frac{1}{1 - \zeta_{s_i} / \zeta_{s_k}}} (J_{k,j})^{\frac{1}{1 - \zeta_{s_k} / \zeta_{s_i}}} \quad (8)$$

Where $J_{i,j}$ corresponds to the normalized intensity at frequency i for $r=r_j$. The advantages of this inversion are immediate. First, the boundary condition $C_1 = J_1$ at the first gate is no longer necessary to perform the inversion. The absence of integrals eliminates the errors caused by their numerical estimates. The propagation of the local errors via the integrals disappears. As a result, the local concentration estimations are independent from all others.

1.4 Results

Figure 1 shows an example of the inverted suspension concentration profile in an Oscillating Grid Turbulence (OGT) experiment conducted at LEGI Grenoble. The suspension is constituted of fine sand particles of mean diameter equal to 126 μ m. The vertically oscillating grid is located at 35cm from the transducer. The generated suspension is in a steady equilibrium state meaning that the mean particle settling flux is in balance with the mean ascendant turbulent erosion flux. The transducer is aligned with the vertical direction being normal to the grid plane.

The three inversion methods have been applied to the acquired mean profiles of normalized intensity. Previously, all system and acoustical parameters have been determined by a rigorous calibration procedure (Bricault 2006). The acoustically determined suspension profiles have been compared to local measurements obtained with a calibrated OBS (D&A instruments).

All three of the above inversion methods were applied to the acquired mean profiles of normalized intensity after all system and acoustic parameters were determined by a rigorous calibration procedure (Bricault 2006). The results for the iterative and explicit methods are calculated for a carrier frequency of 2 MHz. The bi-frequency inversion uses the frequencies of 1.67MHz and 2Mhz obtained quasi-simultaneously with the same wide-band transducer. The same transducer has been used for the iterative and explicit inversions. The spatial resolution in the vertical direction is set to 3mm with a Pulse Repetition Frequency of 1KHz. 32 consecutive pings (or shots) are averaged together for one incoherent acoustic intensity estimate. This setting allows the resolution of the Taylor micro-scale in the investigated suspension flow (Hurther and Lemmin 2007).

For the results obtained from iterative and explicit methods (Eqs (4) and (6)), the increasing divergence of the estimated concentration profiles from the OBS measurements is obvious (Fig. 1). These trends confirm the previously discussed limitations of the standard inversion methods for high-resolution profiling in highly turbulent suspension flows. The bi-frequency inversion results (Eq.(8)) and the OBS measurements are in good agreement over the entire profile. The bi-frequency inversion results into stable concentration profiles even when intensity attenuation by the suspension is significant throughout the water column.

2. Improving high-resolution velocity estimations using bi-frequency Doppler noise suppression

Velocity profile estimations based on the pulse-to-pulse coherent Doppler phase shifts between the emitted and backscattered acoustic pulse trains are subject to important errors due to inherent Doppler noise in the phase of the backscattered wave (Hurther and Lemmin 2007). The effect on the mean velocity estimation is negligible whereas mean turbulent quantities such as the normal turbulent intensities, the TKE, the turbulent velocity spectra, TKE dissipation rate, are particularly affected (Garbini 1982, Voulgaris and Trowbridge 1998, Hurther and Lemmin 2001, Blanckaert and Lemmin 2006). Starting from the expression of the velocity corresponding to the time derivative of the phase shift between emitted and backscattered acoustic pulse trains (Hurther and Lemmin 2007):

$$V = \frac{k_c}{2\pi} \frac{d}{dt} [\hat{r}(t) + \gamma(t)] = \langle V \rangle(t) + n(t) \quad (9)$$

the phase can be decomposed into the term $\hat{r}(t)$ representing the instantaneous spatially average particle displacement within the sample volume, added to the undesired Doppler phase noise term $\gamma(t)$. The contribution of the noise term in the turbulent spectrum is shown in Fig. 2 (circles) for a carrier frequency at 1.25 MHz in the highly turbulent oscillating grid experience described in section 1.4. The measurement location is at $z/z_0=0.67$ (*i.e.* 8 cm from the center of the grid) using the reference

distance for OGT defined by Matsunaga et al. 1999. The velocity spectra are calculated from the Fourier transform of the temporal autocorrelation function of the velocity signal:

$$S_{VV}(f) = \int_{-\infty}^{+\infty} R_{VV}(\tau) \exp(-i2\pi f\tau) d\tau \quad (10)$$

The parameter npp in Fig. 2 indicates the number of samples over which the consecutive velocity estimations are averaged using the pulse-pair algorithm described in Hurther and Lemmin (2001).

As can be seen in Fig. 2 for $f > 3\text{Hz}$, the slope of the velocity spectra presented by the circles deviates from the expected $-5/3$ slope (dashed line). The lower decay with frequencies above 3 Hz is due to the Doppler noise effect represented by the term γ in Eq. (9). When integrated over the frequency band of the system, this undesired effect results into a velocity variance added to the variance of the particle velocity averaged over the sample volume:

$$\overline{V^2} = \langle V \rangle^2 + \sigma^2 \quad (11)$$

This undesired effect is the principal reason for the limited TKE and TKE dissipation rate measurements in field studies (Garbini 1982, Voulgaris and Trowbridge 1998, Blanckaert and Lemmin 2006, Hurther and Lemmin 2001). As will be shown below, the bi-frequency method reduces this effect and at the same time allows high temporal resolution necessary for reliable TKE dissipation estimations.

The bi-frequency method consists of estimating the quasi-instantaneous velocities with two different carrier frequencies at the same time (for the turbulent scales under investigation) and in co-located same sample volume:

$$V_1(t) = \langle V \rangle(t) + n_1(t) \quad (12)$$

$$V_2(t) = \langle V \rangle(t) + n_2(t)$$

where V_1 and V_2 are the instantaneous velocities measured nearly simultaneously with the carrier frequencies, $f_c=f_1$ and $f_c=f_2$, respectively. Each velocity component is composed of the sum of the same spatially averaged velocity and the respective noise contributions. The time-averaged noise contributions are negligible and therefore $\overline{V_1} = \overline{V_2} = \langle V \rangle$. The white noise characteristics induce the following simplification in the crossed spectrum:

$$S_{V_1V_2} = \int_{-\infty}^{+\infty} R_{\langle V \rangle \langle V \rangle}(\tau) \exp(-i2\pi f\tau) d\tau + \int_{-\infty}^{+\infty} R_{n_1n_2}(\tau) \exp(-i2\pi f\tau) d\tau = S_{\langle V \rangle \langle V \rangle} \quad (13)$$

The associated normal Reynolds stress term can be estimated from the covariance as:

$$\overline{V_1V_2} = \int_0^{+\infty} S_{V_1V_2} df = \overline{V_1^2} - \sigma^2 = \overline{V_2^2} - \sigma^2 = \langle V \rangle^2 \quad (14)$$

where the Doppler noise effect is suppressed. If the above reasoning is correct, the crossed-velocity spectrum should decay with a $-5/3$ slope over a much wider frequency band than the auto-velocity spectra presented in Fig. 2. The $-5/3$ slope should be constant until it reaches a frequency limit beyond which it should decay faster because of spatial averaging effects. The turbulent cross-spectrum is represented by triangles in Fig. 2 for comparison with the turbulent auto-spectrum. Both spectra are in good agreement up to 3 Hz. The corrected cross-spectrum preserves a $-5/3$ slope in the inertial subrange until a frequency close to 20Hz. For frequencies above this limit, the spectrum decays with a rate higher than the typical Kolmogorov trend due to spatial averaging effects.

The effect of the bi-frequency Doppler noise suppression method on the mean TKE profile and the TKE dissipation rate is shown in Figs. 3a and 3b, respectively. The bi-frequency method can be compared to the Doppler noise suppression method proposed by Garbini *et al.* (1982) where the crossed spectrum is calculated from the velocity signals at two consecutive locations in the profile:

$$S_{V_1^z V_1^{z+1}} = S_{\langle V \rangle^z \langle V \rangle^{z+1}} \text{ assuming } S_{n_1^z n_1^{z+1}} = 0.$$

The bi-frequency method is tested for frequency shifts of 180KHz and 240KHz between the two carrier frequencies. All measurements are compared to the semi-theoretical models for normalized TKE and TKE dissipation rate valid in highly turbulent OGT (Matsunaga *et al.* 1999).

For both quantities (Figs. 3a and 3b), good agreement is found between the theoretical model (black line) and the two corrected profiles using bi-frequency suppression. The Garbini method underestimates the quantities, because the TKE contained in the isotropic turbulent flow scales of size smaller than the distance separating two consecutive sample volumes is also suppressed. The standard mono-frequency estimate based on the auto-spectrum reveals important noise contributions throughout the profile.

3. Acoustic profiling of turbulent erosion flux

In order to test the capabilities of the ABS in simultaneous and co-located velocity and suspension concentration measurements at turbulent scales (settings at 32 Hz and 3mm), mean turbulent erosion flux versus mean sediment concentration were calculated from data collected in a fully turbulent open-channel suspension flow at EPFL Lausanne (Bricault 2006). For the same particles, the flow conditions were varied over a wide range of flow discharge, Reynolds number, Shields number and relative bed roughness. The slope of the obtained curves has been compared to the settling velocity calculated by the modified Stokes formula valid in turbulent flows (Soulsby 1998). Figs. 4a, 4b and 4c show the results for three different flow conditions. We obtained a good linearity between ascendant mean erosion flux and the mean sediment concentration for all the points in the three profiles and the slopes of the fitted curves are in very good agreement for all flow conditions. Finally, the correspondence with the theoretical value of 3.9 mm/s for the settling velocity is encouraging.

4. Conclusion

This study proposes two novel bi-frequency methods to perform quasi-simultaneous and co-located velocity and suspension concentration profiling at turbulent scales using Acoustic Backscattering Systems working in the MHz range. The first method improves the stability of the inverted suspension concentration profile in situation where intensity attenuation due to sediments cannot be ignored such as found in highly turbulent benthic regions. However, the method is currently still limited to suspensions with mono-dispersed size distributions. The second method allows for an effective suppression of the Doppler noise contribution in the turbulent inertial subrange using the de-correlation of the Doppler noise at two slightly different ultrasound frequencies. As a result, profiles of mean turbulent quantities such as normal intensities, TKE, turbulent spectra, TKE dissipation rates can be estimated more accurately. Finally, the ABS ability to combine velocity and concentration profiling is demonstrated by estimating turbulent erosion flux in highly turbulent suspension flows.

Acknowledgements

This study has been supported partially by the European commission (FP6) under the grant HYDRALAB III-SANDS and the French national program LEFE-IDAO. The technical assistance of J.-M. Barnoud, and C. Perrinjaquet is greatly appreciated.

References

- Admiraal, D.M., and Garcia, M.H. (2000). "Laboratory measurement of suspended sediment concentration using an Acoustic Concentration Profiler (ACP)", *Experiments in Fluids*, 28, 116–127
- Betteridge, K.F.E., Bell, P.S., Thorne, P.D., Williams, J.J. (2006). "Evaluation of a Triple-Axis Coherent Doppler Velocity Profiler for Measuring Near-Bed Flow: A Field Study". *Journal of Atmospheric and Oceanic Technology*, 23(1), 90-106.
- Blanckaert, K., and de Vriend, H.J. (2004). "Secondary flow in sharp open-channel bends", *Journal of Fluid Mechanics*, 498, 353-380.
- Blanckaert, K., and de Vriend, H.J. (2005). "Turbulence structure in sharp open-channel bends", *Journal of Fluid Mechanics*, 536, 27-48
- Blanckaert, K., and Lemmin, U. (2006). "Means of noise reduction in acoustic turbulence measurements", *Journal of Hydraulic research*, 44(1), 3-17

- Bricault, M. (2006) Rétrodiffusion acoustique par une suspension en milieu turbulent: application à la mesure de profils de concentration pour l'étude de processus hydro-sédimentaires. Doctoral Thesis, INP Grenoble, France.
- Elgar S., Raubenheimer, B., and Guza, R.T. (2005). "Quality control of acoustic Doppler velocimeter data in the surfzone", *Measurement Science and Technology*, 16, 1889-1893
- Fugate, D.C., and Friedrichs, C.T. (2002). "Determining Concentration and Fall Velocity of Estuarine Particle Populations using ADV, OBS and LISST." *Continental Shelf Research*, 22, 1867-1886
- Garbini, J.L., Forster, F.K. and Jorgensen, J.E. (1982). "Measurement of fluid turbulence based on pulsed ultrasound techniques. Part 1. Analysis." *Journal of Fluids Mechanics*, 118, 445-470
- Gilboy, T.P., Dickey, T.D., Sigurdson, D.E., YU, X., and Manov, D. (2000). "An intercomparison of current measurements using a vector measuring current meter, an acoustic Doppler current profiler, and a recently developed acoustic current meter." *Journal of Atmospheric and Oceanic Technology*, 17, 561-574.
- Hamilton, L.J., Shi, Z., and Zhang S.Y. (1998). "Acoustic backscatter measurements of estuarine suspended cohesive sediment concentration profiles", *Journal of Coastal Research*, 14(4), 1213-1224
- Hurther, D., and Lemmin, U. (2000). "Shear stress statistics and wall similarity analysis in turbulent boundary layers using a high-resolution 3-D ADVP : Ocean current measurement". *IEEE, Journal of Oceanic Engineering*, 25(4), 446-457
- Hurther, D., and Lemmin, U. (2003). "Turbulent particle flux and momentum statistics in suspension flow." *Water Resources Research*, 39(5), 1139
- Hurther D., Lemmin U. et E.A. Terray (2007). Turbulent transport in the outer region of rough wall open-channel flows: the contribution of Large Coherent Shear Stress Structures (LC3S). *Journal of Fluid Mechanics* 574, 465-493
- Hurther D. and Lemmin U. (2007). Improved turbulence profiling with field adapted Acoustic Doppler Velocimeters using a bi-frequency Doppler noise suppression method. Accepted for publication in *J. of Atmos. and Oceanic Technol.*
- Kim, S.C., Friedrichs, C.T., Maa, J.P.Y., and Wright, L.D. (2000). "Estimating bottom stress in a tidal boundary layer from acoustic Doppler velocimeter data". *J. Hydraulic Eng.* 126, 399-406.
- Lane, S., Biron, P.M., Bradbrook, K.F., Butler, J.B., Chandler, J.H., Crowell, M.D., McLelland, S.J., Richards, K.S., Roy, A.G. (1998). "Three-dimensional measurement of river channel flow processes using acoustic Doppler velocimetry." *Earth Surf. Processes Landforms*, 23, 1247-1267
- Lee, T.H., Hanes, D.M. (1995.) Direct inversion method to measure the concentration profile of suspended particles using backscattered sound. *Journal of Geophysical Research* 100 (C2): 2649-2657
- López, F., and Garcia, M.H. (1999). "Wall similarity in turbulent open-channel flow". *J. Eng. Mech.*, 125, 789-796
- Matsunaga, N., Y. Sugihara, T. Komatsu, and A. Masuda (1999), Quantitative properties of oscillating-grid turbulence in a homogeneous fluid. *Fluid Dynamic Research*, 25, 147-165
- Nikora, V.I., and Goring D.G. (2000). "Flow turbulence over fixed and weakly mobile gravel beds." *Journal of Hydraulic Engineering*, 126, 679-690
- Shen, C., and Lemmin, U. (1999). "Application of an acoustic particle flux profiler in particle-laden open-channel flow". *Journal of Hydraulic Research*, 37(3), 407-419
- Soulsby, R.L., 1997. Dynamics of Marine Sands, a manual for practical applications. *Thomas Telford, England*
- Thorne, P.D., Hardcastle, P.J., Soulsby, R.L. (1993). Analysis of acoustic measurements of suspended sediments. *Journal of Geophysical Research* 98 (C1): 899-910
- Thorne, P.D., Hanes, D. M. (2002), A review of acoustic measurement of small-scale sediment processes. *Cont. Shelf Res.* 22, 603-632.
- Voulgaris, G, and Trowbridge, JH. (1998). "Evaluation of the acoustic Doppler velocimeter (ADV) for turbulence measurements." *Journal of Atmospheric and Oceanic Technology*, 15, 272-289

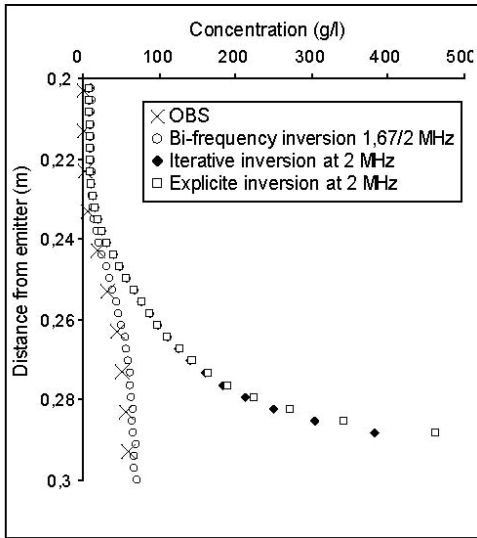


Fig.1 Inverted sediment concentration profiles

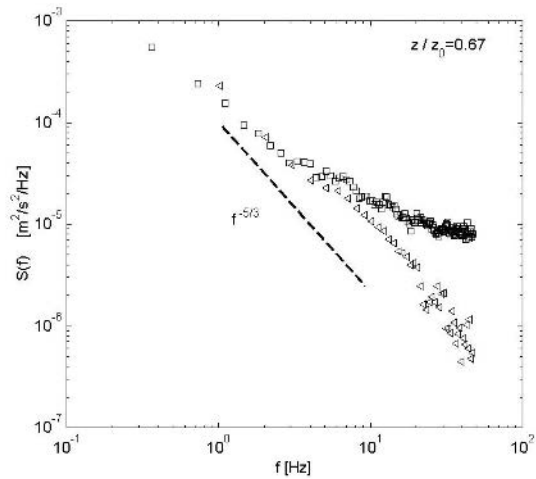


Fig 2. Turbulent velocity spectrum estimation using a standard mono-frequency ADVP and a bi-frequency ADVP

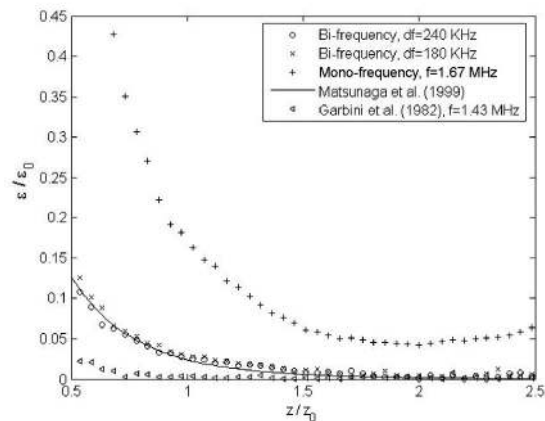
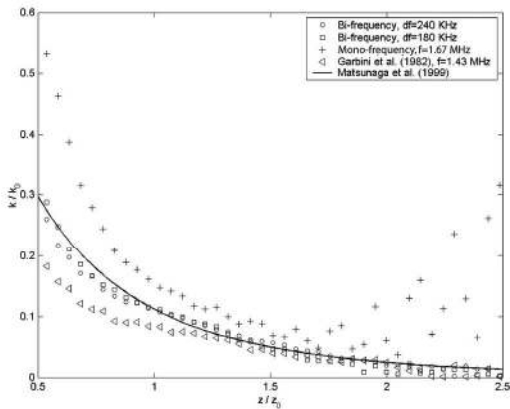


Fig.3 Coherent ADVP measurements of (a) normalized TKE and (b) normalized TKE dissipation rate profiles in an Oscillating Grid Turbulence experiment.

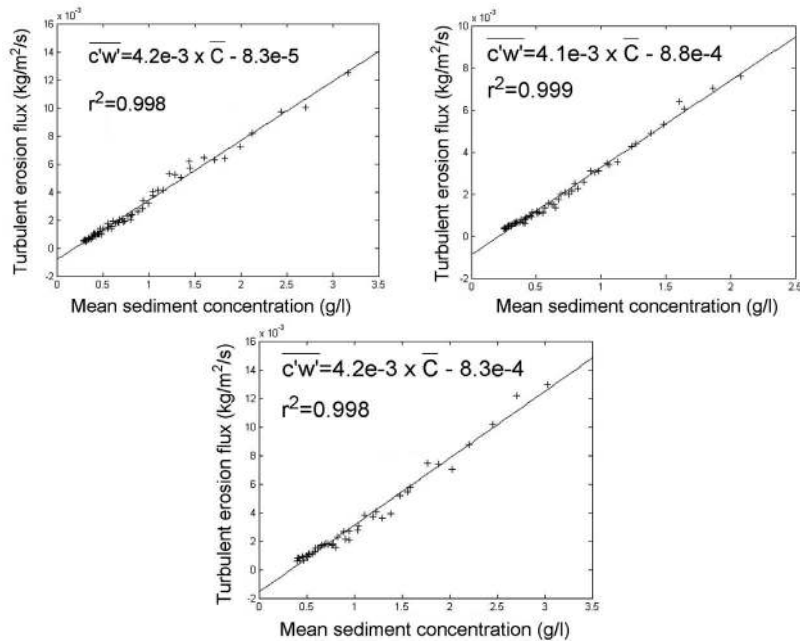


Fig.4 (a) (b) (c) Mean erosion flux versus mean sediment concentration obtained for three different flow conditions (but same sediments) in the benthic region of highly turbulent open-channel suspension flows.